DEVELOPMENT AND OPERATION OF SEISMIC OBSERVATION SYSTEM IN DEEP BOREHOLE

Y. MAMADA[1], G. KOBAYASHI[1], S. WADA[2], K. ARAI[2], K. FUJII[2] and M. SAKURAI[3]

[1] Regulatory Standard and Research Department, Secretariat of Nuclear Regulation Authority (S/NRA/R), Tokyo, Japan

[2] Tokyo Sokushin Corporation, Tokyo, Japan

[3] Oyo Corporation, Ibaraki, Japan

Email contact of main author: yutaka_mamada@nsr.go.jp

Abstract. It was found that the thick sedimentary structure enabled an amplification effect of ground motion during the Niigataken Chuetsu-oki earthquake in 2007. In addition, an attenuation effect from the deep basement is important to predict ground motion on the ground surface. Evaluation of amplification and attenuation effects from the deep basement is one of the important issues to define design basis ground motion for nuclear power plants. To solve such issues, we started the project to perform seismic observation in a deep borehole up to 3000 meters depth in Kashiwazaki city, Japan. In this project, we developed seismic observation tools. The remarkable characteristics of the tools are the following: (1) a seismometer recordable under high temperature (150 degrees Celsius) and pressure (a pressure of 300 atmospheres), (2) a seismometer with wide dynamic range and relatively broad band frequency ranges, and (3) a cascade-type borehole seismometer which enables multi-depth seismic observation in one borehole. This observation system began to be operated since 2012 and has collected many ground motion records during about one and a half years. This paper presents this observation system including the developed tools for seismic observation in a deep borehole and the operation performance of the system.

Key Words: Seismic observation system, Deep borehole, Design basis ground motion, Site effect

1. INTRODUCTION

The ground motion observed in the south-western units of Kashiwazaki-Kariwa nuclear power plant far exceeded the design basis ground motion during the Niigataken-Chuetsu oki earthquake in 2007. Its peak ground acceleration was about two times as large as that observed in the north-eastern units which are located only about 1800 m away from the south-western units. Such large difference of ground motion was attributed to an irregular deep underground structure based on the analysis by Japan Nuclear Energy Safety Organization [1]. This made us learn that it is important to comprehend the details of deep underground structures to evaluate strong ground motion correctly. In addition, recent evaluation of ground motion attenuation just under a plant site has been one of the most important issues (e.g. Kobayashi et al., 2011 [2])).

One of the useful methods to understand deep underground structures and attenuation properties of ground motion is to apply vertical array observation down to the seismic basement where amplification and attenuation of ground motion may have little site dependence. We then started a project on seismic observation in a deep borehole in 2009. This project includes site selection for deep borehole observation, application of deep boring technique to selected site, development of observation tools, installation of these tools in deep boreholes and evaluation

of site effect (amplification and attenuation from deep underground) based on seismic data obtained in deep borehole observation. We selected the campus of Niigata Institute of Technology (NIIT site) as the boring site, since the underground structure is similar to that under the Kashiwazaki-Kariwa plant where the seismic basement and geological strata are west-dipping and the seismic basement was expected to be shallower than the other sites around the Kashiwazaki-Kariwa plant. Borehole drilling down to about 3000 m depth was completed in May 2011. The installation process of observation tools was completed in January 2012 and observation has started since June 2012. In this report, firstly, we principally present the development of the observation tools such as the seismometer and installation tool setting the seismometer in the deep borehole. Secondary, we also present the performance of the seismic observation using the developed tools. The results using records from collected this observation system are introduced by Kobayashi and Mamada [3] .

2. OVERVIEW OF OBSERVATION SYSTEM

Figure 1 shows an overview of the developed seismic observation system in a deep borehole. We note that ground motion at a depth shallower than 100 m is supported by supplement seismometers in another shallow borehole. Our system consists of a cascade-type borehole seismometer which enables multi-depth 3-component observation in one borehole. Each seismometer in a deep borehole is designed to be relatively highly sensitive and have a broad dynamic range, so as to enable recording from microtremors to strong motions over a relatively broad-band frequency range (0.2 to 20 Hz). Moreover, a borehole seismometer installed in a deep borehole needs to be high-temperature and pressure resistant because the temperature and water pressure at a depth of 3000 m are about 142 degrees Celsius and 3.0×10^6 kg/m^2, respectively. Here, temperature was directly measured in the borehole and the temperature measured at the depth of each seismometer location is shown in Fig.1. A seismometer with these characteristics had not yet been developed. We then developed one in this project in order to complete observation in deep borehole. Data was continuously recorded with a sampling frequency of 200 Hz. The data was tentatively collected on a PC and transferred to the server in Nuclear Seismic and Structure Research Center on the NIIT campus.

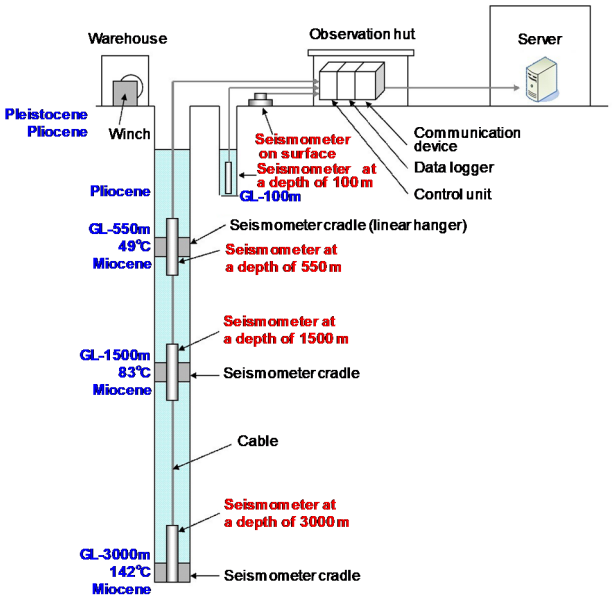

FIG. 1. Overview of seismic observation system in deep borehole

2.1 Design of seismometer

We designed a seismometer to be used under high temperature of about up to 150 degrees Celsius. A seismometer can ordinarily be used under a temperature up to around 50 degrees Celsius at most. This limitation is caused by the electronic parts in a seismometer being susceptible to damage at high temperatures. To avoid this limitation, the seismometer is designed to separate the electronic parts from the pendulum, so that the electronic parts are set on ground surface (see Fig. 2). This design permits us to calibrate the frequency response of the seismometer without rolling it up from deep borehole. In addition, the seismometer is designed to be covered with a high pressure resistant titanium probe to protect it from high pressure (up to 3.0×10^6 kg/m^2).

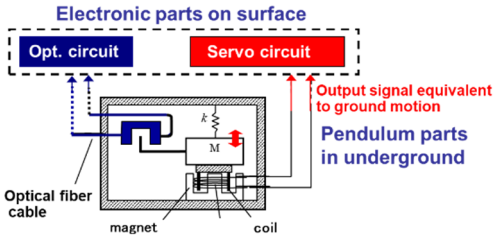

FIG. 2. Design of seismometer. The developed seismometer could be operated as both a servo-type sensor and a pendulum-type sensor. Electronic parts including the optical circuit and servo circuit were designed to be set on the ground surface.

Another characteristic of the developed seismometer is the acceleration level of the recordable range (Fig.3). The developed seismometer can record strong seismic motion which cannot be recorded by the highly sensitive velocity sensor STS2. The developed seismometer also has relative high sensitivity in the low frequency band (lower than 10 Hz) comparing the accelerometer, although the sensitivity is not as high as that of the STS2. One more remarkable characteristic is that three depth seismometers are linked by one cable so that each depth seismometer can be installed at each depth in one borehole. During the seismometer installation or removing, large tension (more than 3000 kg) acts on the cable. We then attached a tension member to strengthen the cable for large tension. The cross-section of the final designed cable is shown in Fig. 4.

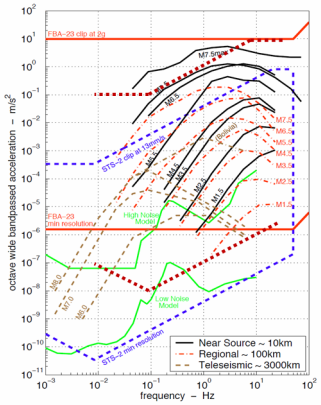

FIG. 3. Recordable range of seismometers on frequency domain. The areas enclosed by brown, red and blue lines show the recordable ranges of the developed velocity seismometer, the typical standard accelerometer FBA-23 and the velocity sensor STS2, respectively. The typical spectra from various types of earthquakes with different magnitudes are also shown. This figure is made by modifying that of Clinton [4].

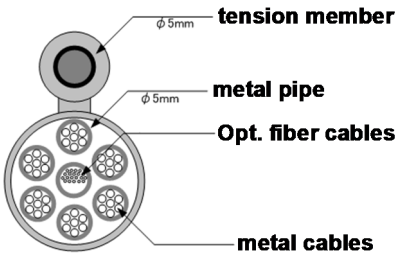

FIG. 4. Cross-section of designed cable

2.2 Installation method of seismometer into deep borehole

Our design requires to install a seismometer at the middle point in a borehole. In order to fix a seismometer in a borehole, a liner-hanger, which was used for oil drilling to fix casing pipe at any point in the borehole, was applied. In other words, casing pipe in which a seismometer cradle attached was hung by liner-hanger, and the seismometer cradle was fixed by the liner-hanger at any point in the borehole. The azimuthal direction of the seismometer in the horizontal component was determined by correlation analysis of surface waves observed at the surface and in the borehole after installation.

3. DEVELOPMENT OF OBSERVATION TOOLS

3.1 Outline of performance tests

The developed tools in this project were checked by various laboratory tests and field experiments. Table 1 is a list of principal tests and we show the results of several principal tests in this section.

TABLE 1: A LIST OF PRINCIPAL PERFORMANCE TESTS.

Tools	Item to be checked	Performance test	Test conditions
Sesimometer Resistance to high temperature and pressure	Temperature: 150℃	Heating test up to 200℃ by electric furnace	Continuous 32 days
	Pressure: 30MPa	Pressurization test of seismometer probe	Up to 50MPa
	Acceleration test for high temperature	Periodic heating and cooling test between −10℃ and 120℃	heating: a half day cooling: a half day during 10 days
	Test against high temperature and pressure	Long-term experiment in borehole (120℃,10MPa)	3 months under 120℃ and 10MPa

TABLE 1: (continued).

Tools	Item to be checked	Performance test	Test conditions
Seismometer Sensor Characteristics	Frequency response: 0.1 to 50 Hz (amplitude flat)	Check by test signal (Comparison of input- and output- signal)	
	Resolution: 10^{-5} gal at 1Hz	Field experiment under low noise area. Comparing microtremor records by reference (VSE15D) and developed seismometers.	
	Maximum Acceleration: 1000 gal	Laboratory test by shaking table	
Cable	Tensile strength: 3000kg	Tensile loading test up to 3000kg for cable unit (including cable head)	
	Crosstalk test for multi-channel signals	Check of signal interaction for any pair of channels	
Seismometer cradle	Stable contact to borehole wall for frequency ranges 0.1 to 50 Hz	Comparison of records by seismometer installed in bottom and middle point in test borehole	

3.2 Performance test of seismometer

Performance tests to check the high sensitivity and applicability to strong seismic motion are described in this section. Figure 5 shows the frequency response of the developed seismometer (used as velocity-type sensor). Amplitude response is almost flat (within 3dB) in the frequency range of 0.1 to 50 Hz. Applicability to strong seismic motion was confirmed by a shaking table test. The developed seismometer was vibrated from 0 to 1000 cm/s^2 on a shaking table and we confirmed output from the seismometer was proportional to the exciting acceleration from the shaking table.

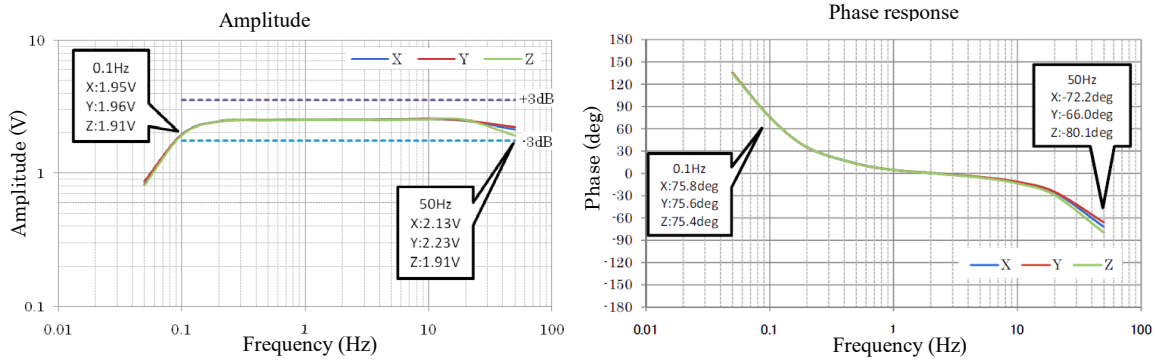

FIG. 5. Frequency response of developed seismometer. Each curve represents frequency response when used as a velocity-type sensor.

Sensitivity was checked by microtremor records which were obtained under a very low noise environment (1.0×10^{-5} to 1.0×10^{-4} cm/s^2 at frequency ranges from 0.1 to 10 Hz). Microtremor records were obtained in the same field by two seismometers (the developed seismometer and reference seismometer VSE-15C) and spectra from these seismometers were compared. The results show that these spectra are almost the same at frequency ranges from 0.1 to 10 Hz (Fig. 6). Since electric noise exceeds the microtremor level at above 10 Hz, the seismometer cannot detect such small signal. However, the spectra from earthquake records which exceeded 1mgal were almost the same at frequencies up to 50 Hz.

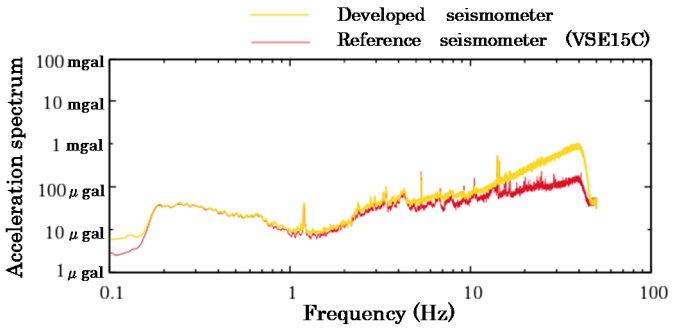

FIG. 6. Comparison of microtremor spectra recorded by the developed seismometer and reference seismometer (VSE15C). The spectrum is evaluated by root mean squares over 1/3 octave frequency band.

3.3 Performance test of liner-hanger

The casing pipe with the seismometer cradle is fixed to the borehole by a liner-hanger (Fig. 7) in this observation system. Therefore, the fixing strength between the liner-hanger and the casing pipe is important to record ground motion precisely. In order to confirm the strength, we set the casing pipe to be installed in the borehole on the ground surface, and fixed another casing pipe with a seismometer cradle to the former casing pipe by a liner-hanger. Using this test equipment, tensile force of up to about 20.0×10^3 kg in the vertical direction was loaded at the casing pipe fixed by the liner-hanger. Significant displacement of the casing pipe was not found in this test. Next, tensile force of up to about 2.5×10^3 kg in the horizontal direction was loaded. In this case too, significant displacement was not found. These results show the casing pipe with the seismometer cradle can be fixed adequately.

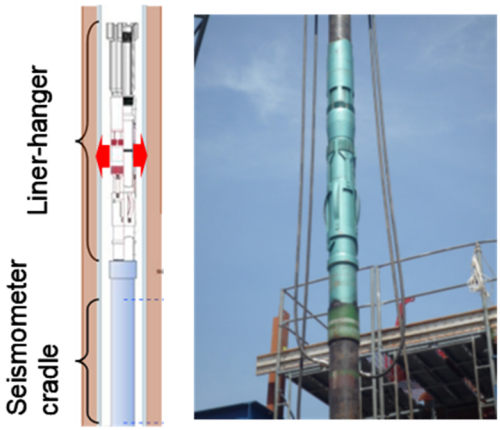

FIG. 7. Schematic illustration of liner-hanger (left) and photograph of it (right). At the target depth, the liner-hanger can be fixed to the casing pipe by increasing its diameter (shown by red arrows).

In addition, we checked seismograms recorded by the seismometer fixed in the borehole using the liner-hanger. A reference seismometer was installed in the bottom of the borehole with a depth of 40 m. The developed seismometer was fixed at the same depth (40 m) in a borehole with a depth of 70 m using a liner-hanger. The horizontal distance between the two boreholes is about 10 m. Seismograms recorded by both seismometers were compared and we confirmed that the spectra from both seismograms were almost the same at a frequency range of 0.1 to 10 Hz. At higher than 10 Hz, significant difference was found only in horizontal component seismograms. This may be due to high frequency noise caused by mechanical problems involving the liner-hanger in this observation system.

3.4 Resistance experiment under high temperature and pressure

We describe the high temperature and pressure resistance of the developed seismometer in this section. The applicability to high temperature and pressure was checked by both laboratory tests and field experiment. It is difficult for our system to check applicability to both high temperature and pressure in a simultaneous laboratory test. Therefore, firstly, applicability to high temperature and pressure were tested independently in laboratory tests. Secondly, we checked applicability to high temperature and pressure loaded simultaneously in a long-term field experiment.

Principal laboratory tests consisted of a high temperature resistance test using an electric furnace, a high temperature acceleration test using an electric furnace and a high pressure resistance test using a hyperbaric chamber. The high temperature resistance test was performed by setting the seismometer in an electric furnace, heating to 200 degrees Celsius, and keeping the temperature for 32 days. After heating, the frequency response of the seismometer was checked, and we confirmed there was no significant difference in response before and after heating the seismometer. The high temperature acceleration test was performed by heating the seismometer to 120 degrees Celsius for a half day and cooling it to -10 degrees for a half day using an electric furnace. This test was repeated for 10 days. We confirmed that there was no significant difference in spectra before and after the test. The high pressure test used a high pressure vessel, covering the seismometer completely with the vessel. The vessel was compressed up to 5.0×10^6 kg/m^2 in a hyperbaric chamber for 3 hours. There was no significant deformation of the vessel and water injection into the vessel, and it was confirmed that the vessel has resistance to high pressure up to 5.0×10^6 kg/m^2

The long-term experiment under high temperature and pressure was performed using a test borehole. The temperature and pressure at a depth of 1000 m were about 120 degrees Celsius and 1.0×10^6 kg/m^2, respectively. We note that these values are smaller than those of the NIIT site. However, this site is the only site where we can test under an environment of both high temperature and pressure. The experiment period was three months. Although the temperature in this borehole becomes about 120 degrees Celsius at a depth of 1000m, the borehole has an inclination of more than 40 degree at a depth of greater than 1000 m. As a result, we cannot collect normal records using the seismometer in this borehole. We then set the seismometer at a depth of 1000 m in the borehole, and every 1 month later we rolled it up to the ground surface and recorded microtremors on the ground surface. This process was repeated three times for three months. The response spectra of microtremors were compared with those recorded by a reference seismometer. As a result, significant variation of response spectra was not found through the experiment period.

4. DATA ACQUISITION

Installation operation was started on Dec. 8, 2011, after checking all tests mentioned above and it was completed on Jan. 23, 2012. After installation, several seismometer calibrations (for example, calibration of frequency response and identification of direction of horizontal seismometer) were successively performed.

Far off the south-east coast of Hokkaido earthquake (Mj6.9) on March 14, 2012	Off the west coast of northern Sumatra earthquake (M8.6) on April 11, 2012

Correlation coefficients between the records on ground surface and at depth of 100 m

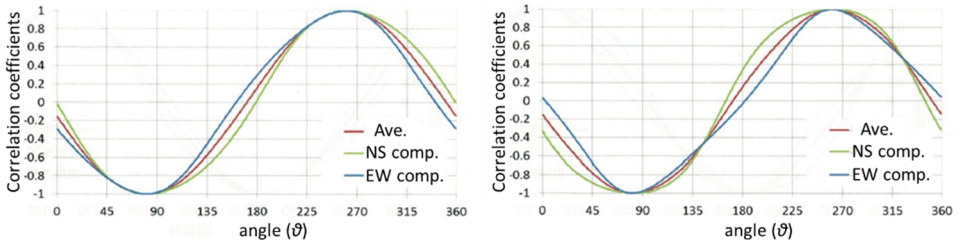

Correlation coefficients between the records on ground surface and at depth of 550 m

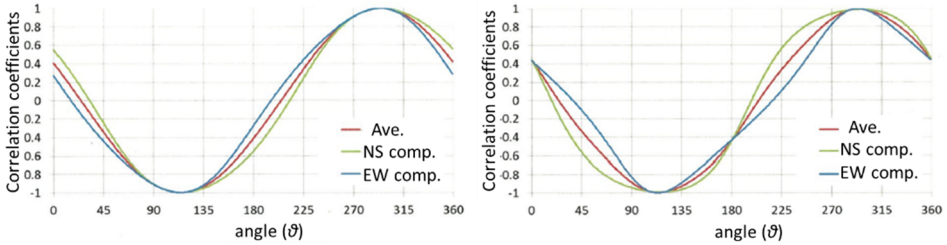

Correlation coefficients between the records at depths of 550 and 1500 meters

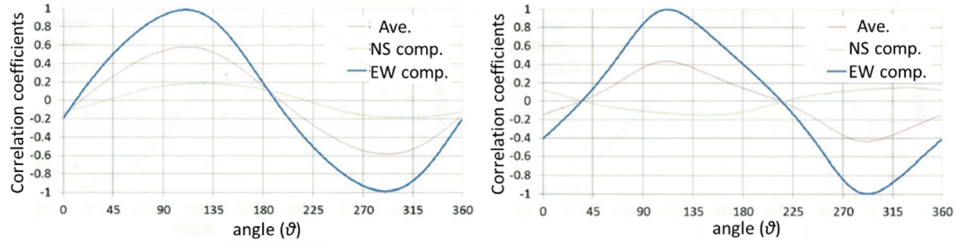

Correlation coefficients between the records at depths of 550 and 3000 meters

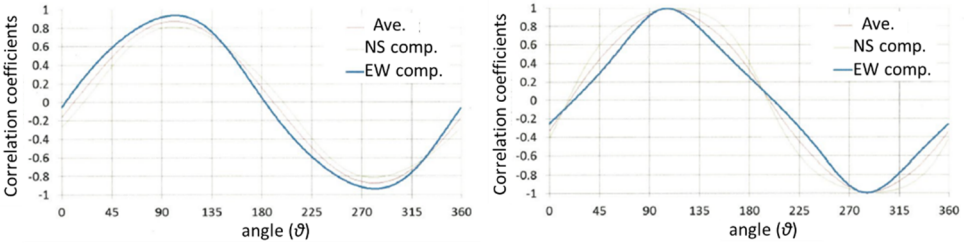

FIG. 8. Correlation coefficients as a function of angle θ for two earthquakes. Magnitude for events on March 14, 2012, and April 11, 2012, were determined by the Japan Meteorological Agency and the U.S. Geological Survey, respectively.

We identified the direction of the horizontal seismometer in each depth by measuring correlation of surface waves recorded between on the surface and at depth for two regional earthquakes (in this case, the Far off the south-east coast of Hokkaido earthquake on March 14, 2012 (Mj6.9) and the Off the west coast of northern Sumatra earthquake on April 11, 2012 (M8.6)). Horizontal velocity seismograms filtered at 8 to 10 seconds were used to measure correlation. Correlation coefficients of surface waves recorded between on the ground surface and at depths of 100 and 550 meters were calculated. After identifying the direction of the seismometers at depths of 100 and 550 meters, the directions of the seismometers at 1500 and 3000 meters were measured by correlation coefficients between at a depth of 550 m and at 1500 and 3000 meters, respectively. Here, the correlation coefficient was estimated as follows. Since the angle between the directions of the two horizontal component seismometers was 90 degrees, assuming the azimuthal angle of the horizontal component for the seismometer at depth as θ measured from north direction, we transformed to seismograms in north-south (NS) and east-west (EW) direction from the original horizontal seismograms. Next, we calculated the correlation coefficients between the two seismograms. One is a seismogram recorded on the ground surface and another at depth. Correlation coefficients are estimated for seismograms in both the NS and EW directions. Fig.8 shows the correlation coefficient as a function of θ. The direction of the seismometers at depth was identified by θ_0 which maximizes the correlation coefficients. Here, θ_0 was estimated for seismograms in the NS and EW directions for two earthquakes, and we determined the directions of the seismometers by averaging over four values of θ_0. The results of the identified direction of the seismometer at each depth are shown in Fig. 9.

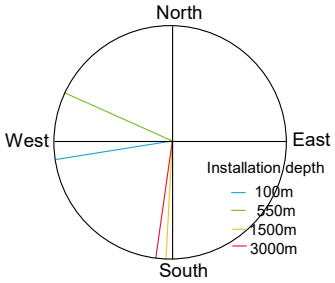

Installation depth of seismometer	Azimuthial angle (degree) (clockwise from the north)
100 m	261
550m	294
1500m	182
3000m	189

FIG. 9. Azimuthal angles identified by surface wave analysis

The observation has started since June 2012 and continuous records have been collected. These records include some moderate to great earthquakes, for example, aftershocks of the 2011 off the Pacific coast of Tohoku Earthquake that occurred on the Pacific coast and inland earthquakes. Figure 10 shows an example of seismograms. Table 2 shows the collected large events whose acceleration records are greater than 1 cm/s^2. Such data have a potential to be used for precise evaluation of ground motion under a complex structure.

TABLE 2: A LISTS OF COLLECTED LARGE EVENTS. HYPOCENTERS ARE DETERMINED BY THE NATIONAL RESEARCH INSTITUTE FOR EARTH SCIENCE AND DISASTER PREVENTION.

Date	Time (JST)	Lat.	Long.	Dep.	Mj
Jul. 10, 2012	12 48 57.44	36.831	138.388	8.5	5.2
Jul. 14, 2012	13 04 30.14	36.828	138.367	7.8	3.7
Oct. 18, 2012	00 01 40.79	37.028	138.709	7.1	4.2
Oct. 18, 2012	01 16 43.66	37.028	138.701	8	3.3
Nov. 20, 2012	01 22 48.24	37.617	138.578	16.6	3.6
Dec. 05, 2012	08 02 52.50	37.247	138.944	11.3	4.1
Dec. 07, 2012	17 18 30.81	38.02	143.867	49	7.3
Feb. 25, 2013	16 23 53.58	36.874	139.413	2.8	6.3
Jun. 07, 2013	22 29 21.09	37.173	138.177	10.7	3.8

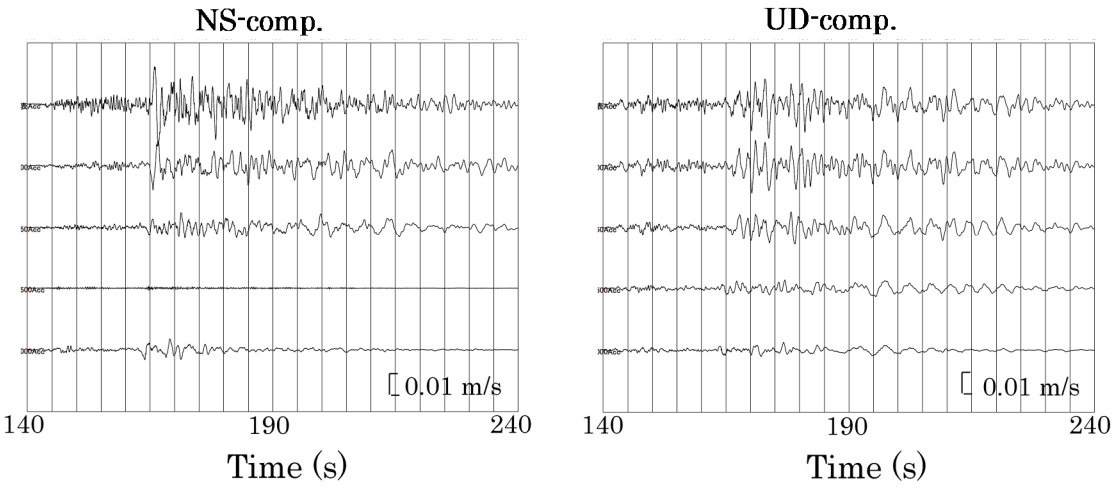

FIG. 10. Example of seismogram. Each trace shows the seismogram at depths of 0, 100, 550, 1500 and 3000 m from top to bottom, respectively. We note that the horizontal component seismometer at a depth of 1500 m has shown little signal since February 2, 2012. This may be due to the deformation of the cable at just below the seismometer cradle at around a depth of 550 m, according to a detailed check of our observation system.

5. OPERATION OF OBSERVATION SYSTEM

There are no seismometer operation experiences under such severe condition with a high temperature of about 140 degrees Celsius. After installation of the seismometer into the borehole, we performed several checks (for example, sensor sensitivity, energy loss of propagating light waves along optical fiber cable) basically at every three months to maintain the quality of seismic records. Table 3 shows the performance of observation. In this table, the principal event which occurred in the observation period and operation conditions for each seismometer are represented. Several small troubles occurred through the observation period. However, most of them were resolved by periodic maintenance. Severe troubles occurred just after the installation, Feb, 2013, and Nov. 2013. Sensors for X- and Y- components at a depth of 1500 m had trouble in the servo circuit during the installation process. Here, the X- and Y-components represent the two directions of the horizontal seismometers. The direction of the Y-components is rotated by 90 degrees clockwise, measured from the direction of the X-component on the horizontal plane. Sensors for the Y-component could be operated as a pendulum-type seismometer using an optical circuit (see Fig.2). On the other hand, the sensor for the X-component could not be operated and we stopped operation of this sensor. On Feb, 2013, the sensor for the Z-component (in other words, vertical component) at a depth of 1500 m had mechanical trouble related to the pendulum, and we could not operate this sensor. On Nov. 2013, recording for all components at a depth of 3000 m stopped. Only the sensor for the Y-component at a depth of 3000m could be operated as a pendulum-type seismometer using the optical circuit. Recording of this sensor was re-started after sensitivity calibration in February 2014. However, the sensors for the X- and Z- components could not be recovered.

Sensitivity check was performed by measuring the output signal against the electric input signal (2.5 V) which is equivalent to a velocity level of 1.0 cm/s. The results are shown in Fig.11. The lack of data for the X- and Y- components at a depth of 1500 m are due to trouble of a part in the sensors. Although recording for the Y-components could be re-started, sensitivity check could not be performed, because of the trouble in the circuit to be used for

sensitivity check. In addition, recording of the X- and Y- components at a depth of 3000 m stopped in Nov. 2013; therefore, we terminated sensitivity check hereafter. Figure 11 shows that the sensitivity for almost all seismometers is stable during about one and half years after the beginning of observation except for the X-components at depth of 3000 m, for which sensitivity became unstable three months from the beginning of observation. Although we tried sensitivity improvement for this component in maintenance every three months, a large sensitivity change continued and did not improve. On the other hand, sensitivity for the Y- and Z- components at the same depth which is operated as a servo-type sensor has been continuously stable for at least one and half years. We note that our sensor is more sensitive to energy loss of light waves propagating in optical fiber cable when operated as a pendulum-type sensor than as a servo-type due to the mechanical structure of this seismometer. Periodic checking of light intensity propagating along the optical cable shows that the energy loss in optical fiber cable, especially extending to a depth of 3000 m, increases as time elapses from the beginning of observation. This may be due to degradation of optical fiber cable due to thermal effect, it being exposed to high temperatures of above 140 degrees Celsius.

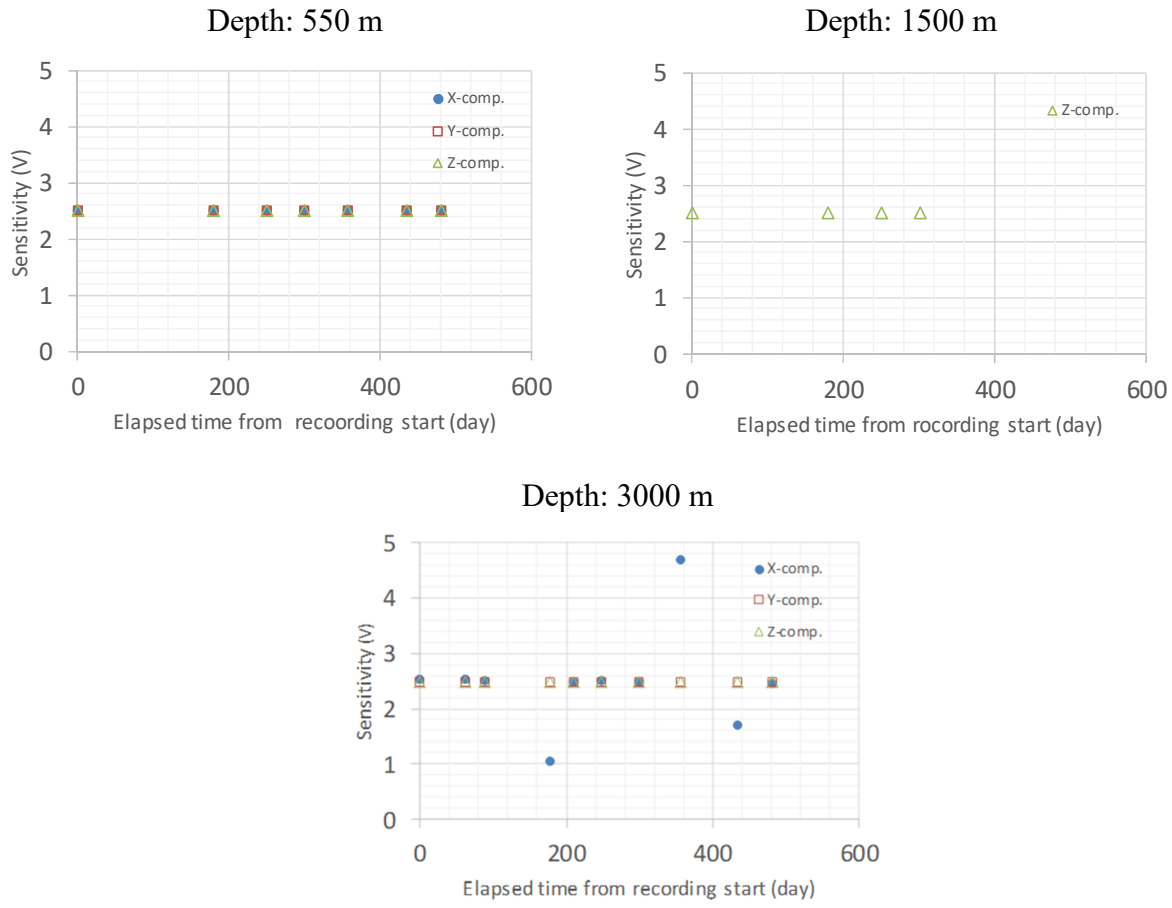

FIG. 11. Results of sensitivity check. Each panel shows the sensitivity against elapsed time from the recording start for the sensors located at depths of 550, 1500 and 3000 meters.

TABLE 3: PERFORMANCE OF OBSERVATION.

Date	Condition of seismometers	Pricipal event	550m			1500m			3000m		
			X	Y	Z	X	Y	Z	X	Y	Z
Feb. 2012	All seismometers were operated as servo type sensor		○	○	○	×	×	○	○	○	○
Mar. 2012	Operation of seismometer for X-comp. at depth of 1500 m are changed into pendulum-type operation.	Event at far off the south-east coast of Hokkaido (M6.9) Event near Choshi city Event at east far off of Iwate pref.	○	○	○	×	○	○	○	○	○
Apr. 2012		Event at off the east of Fukushima pref. Event off the west coast of northen Sumatra (Mw8.6)	○	○	○	×	○	○	○	○	○
May. 2012	Seismometers for X- and Y-comp. at depth of 3000 m had lower sensitivity. Sensitivity was improved by maintenance.		○	○	○	×	○	○	○	×	×
Jun. 2012	Sensitivity for X- and Y-comp. at depth of 3000 m was improved by maintenance. Calibration completed and formal operation started.		○	○	○	×	○	○	○	○	○
Jul. 2012		Event at northern Nagano pref. Event at boundary of Tochigi and Gunma pref.	○	○	○	×	○	○	○	○	○
Oct. 2012	Recording for Y- comp. at depth of 3000 m stopped.	Event at middle Niigata pref.	○	○	○	×	○	○	○	×	○
Oct. 2012	Recording restarted by maintenance.		○	○	○	×	○	○	○	○	○
Nov. 2012	Recording for X- comp. at depth of 3000 m stopped.	Event off southern Niigata pref.	○	○	○	×	○	○	○	○	○
Dec. 2012	Recording restarted by maintenance.	Event at middle Niigata pref. Event at far east off northern Japan	○	○	○	×	○	○	○	○	○
Jan. 2013	Recording for Z- comp. at depth of 3000 m stopped.		○	○	○	×	○	○	○	○	×
Jan. 2013	Recording restarted by maintenance.		○	○	○	×	○	○	○	○	○
Feb. 2013	Seismometers for Z- comp. at depth of 1500 m had trouble. Recording for Z- comp. at depth of 3000 m stopped.	Event at nothern Tochigi pref.	○	○	○	×	○	×	○	○	×
Mar. 2013	Recording for Z- comp. at depth of 3000 m restarted by maintenance.		○	○	○	×	○	×	○	○	○
Jun. 2013	Recording for Y- comp. at depth of 3000 m stopped.	Event at south-western Niigata pref.	○	○	○	×	○	×	○	×	○
Jul. 2013	Recording restarted by maintenance.		○	○	○	×	○	×	○	○	○
Aug. 2013	Recording for Z- comp. at depth of 550 m has anomaly.		○	○	×	×	○	×	○	○	○
Aug. 2013	Recording for Y- and Z- comp. at depth of 3000 m stopped.		○	○	×	×	○	×	○	×	×
Sep. 2013	Recording for Y- and Z- comp. at depth of 3000 m restarted by maintenance.	Event near the Torishima Island	○	○	○	×	○	×	○	○	○
Oct. 2013		Event at far east off of nothern Honshu, Japan	○	○	○	×	○	×	×	×	×
Nov. 2013	Recording for all comp. at depth of 3000 m stopped.		○	○	○	×	○	×	×	×	×
Feb. 2014	Recording for only Y-comp. at depth of 3000 m restarted by maintenance. Operation of this seismometer was changed into pedulum-type operation.		○	○	○	×	○	×	×	○	×

○ : normal operation, × : operation with trouble or operation stop

6. BACKGROUND NOISE AND SENSOR SENSITIVITY IN DEEP BOREHOLE

One of the interests in deep borehole observation is the level of background noise in seismic records which is a sum of microtremors, electric noise caused by the sensor itself, mechanical noise from the observation system itself and so on. The background noise level in records collected in a borehole is generally expected to be smaller than that on the ground surface. Therefore, data collected in a borehole have advantages in many studies, for example, analyses of source spectrum, propagation characteristics of seismic waves and so on. We then checked the level of background noise at five depths and also discussed the sensitivity of the developed seismometer. Figure 12(a) compares the background noise recorded for the horizontal component (east-west component). The background noise gradually decreases as depth increases up to a depth of 1500 m. On the other hand, the level at a depth of 3000 m is larger than those at depth of the others. Figure 12(b) shows RMS (root-mean-square) amplitude which is estimated from octave wide band-passed acceleration records for background noise at five depth points. The levels at a depth of 0 and 100 meters are almost equivalent. The level at a depth of 550, 1500 and 3000 meters are also equivalent, except the level at the depth of 3000 m at a frequency range higher than about 5 Hz. Noise level rapidly increases at a frequency range higher than 5.0 Hz. This noise may be attributable to the long cable from the surface to the seismometer location at a depth of 3000 m which can be affected by electric noise.

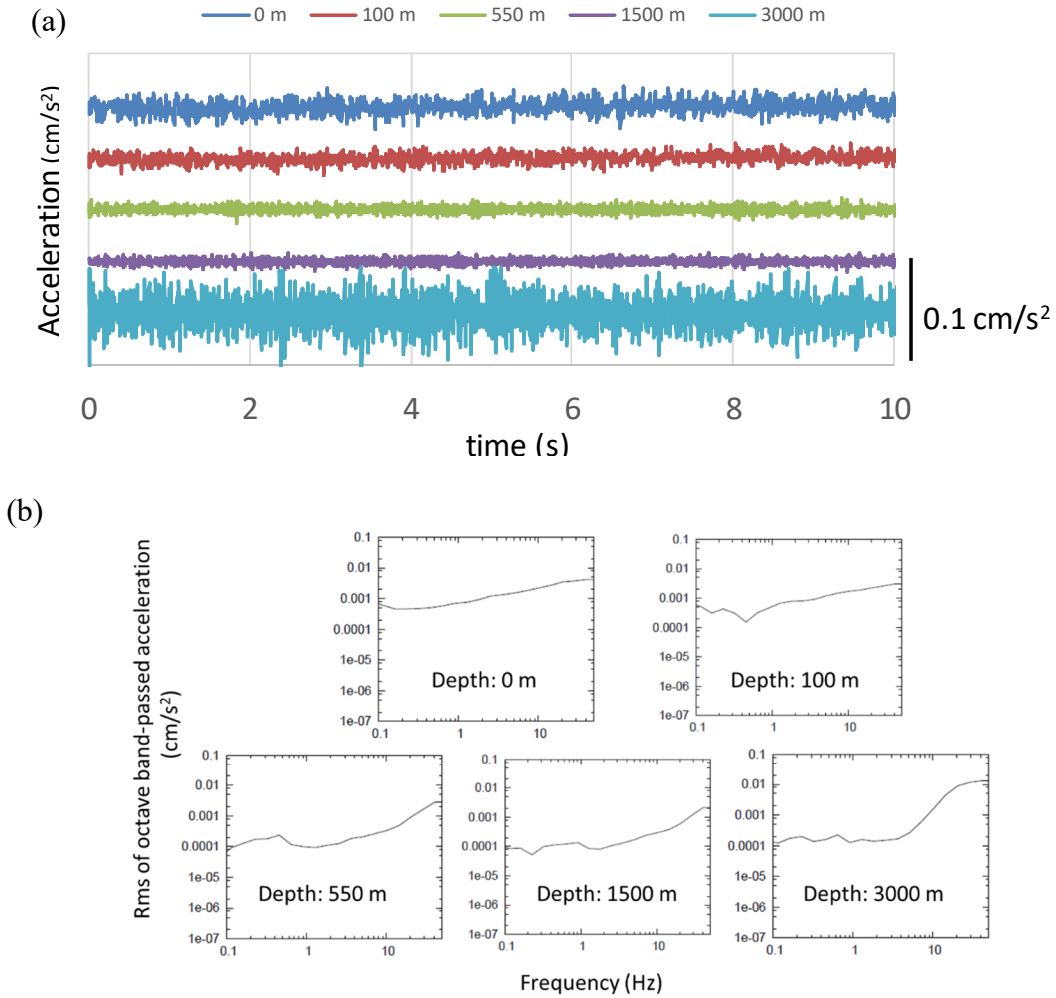

FIG. 12. (a) Acceleration seismograms at five depth points for background noise on 10 July, 2012. (b) Root mean square of octave band-passed acceleration over 10 seconds at five depth points for background noise shown in Fig 12(a).

Comparing Figs.3 and 12(b), we can see background noise is recorded well, since the level is adequately higher than the lower limit of the seismometer recordable range. The level is several times as large as the level of the lower limit. Considering the level of background noise, at depths of 0 and 100 meters, a signal level larger than 1.0×10^{-3} and 1.0×10^{-2} cm/s^2 at a frequency range lower and higher than 10 Hz can be recorded with a good signal/noise level, respectively. At depths of 550 and 1500 meters, a signal level larger than 1.0×10^{-4} and 1.0×10^{-3} cm/s^2 at a frequency range lower and higher than 10 Hz can be recorded. At a depth of 3000 meters, a signal level larger than 1.0×10^{-4} cm/s^2 at lower than 10 Hz can be recorded similar to those at depths of 550 and 1500 meters. However, at higher than 10 Hz, the signal level needs to be larger than 1.0×10^{-2} cm/s^2. Therefore, the actual sensitivity of the seismometer against the input signal at a depth of 3000 m is lower than the other seismometers (at depths of 500 and 1500 meters) at a high frequency range.

7. SUMMARY

We developed seismic observation tools to collect the seismograms which enable us to construct an underground structure with a thick sedimentary structure. The developed tools have remarkable characteristics as follows: (1) a seismometer recordable under high temperature (150 degrees Celsius) and pressure (a pressure of 300 atmospheres), (2) a seismometer with a large dynamic range and relatively broad band frequency ranges, and (3) a cascade-type borehole seismometer which enables multi-depth seismic observation in one borehole. This observation system has been operated since 2012 and enabled us to collect high quality ground motion records during about one and a half years. Seismic records collected by this observation system were used effectively to restrict the uncertainty of underground model. As a result, we constructed fine 3-dimensional shear-wave velocity structure model which is important to evaluate the strong ground motion (Kobayashi and Mamada, 2018 [3]). All seismometers installed at depth were rolled up in February 2017 and this project was completed.

REFERENCES

[1] Japan Nuclear Energy Safety Organization, Report prepared for working group meeting for earthquake, tsunami, geology and ground base in Nuclear and Industrial Safety Agency (NISA) (2008). http://www.meti.go.jp/committee/materials/downloadfiles/g80617a02j.pdf

[2] KOBAYASHI, G., Y. MAMADA and H. TSUTSUMI, Consideration on frequency dependences of near-surface attenuation of S- waves based on vertical array records, *Journal of Japan Association for Earthquake Engineering*, **11,** 1-20, (2011).

[3] KOBAYASHI, G. and Y. MAMADA, Construction of a high-resolution 3-dimensional S-wave velocity structure model based on a joint inversion method integrating various kinds of geological and geophysical data, Paper preparation for IAEA workshop: Best Practices in Physics-based Fault Rupture Models for Seismic Hazard Assessment of Nuclear Installations: issues and challenges towards full Seismic Risk Analysis, (2018).

[4] CLINTON, J. F., Modern Digital Seismology – Instrumentation and small amplitude studies for the engineering world, PhD Thesis, California Institute of Technology. (2004).